Chinese Chemical Letters 35 (2024) 109082

Contents lists available at ScienceDirect

Chinese Chemical Letters

journal homepage: www.elsevier.com/locate/cclet

Structural evolution and zero-field SMM behaviour in ferromagnetically-coupled disk-type Co_7 clusters bearing exclusively end-on azido bridges

Yijia Jiao[a], Yuzhu Li[a], Yuting Zhou[a], Peipei Cen[b], Yi Ding[a], Yan Guo[a], Xiangyu Liu[a,*]

[a] State Key Laboratory of High-efficiency Utilization of Coal and Green Chemical Engineering, College of Chemistry and Chemical Engineering, Ningxia University, Yinchuan 750021, China
[b] College of Public Health, College of Basic Medical Science, Ningxia Medical University, Yinchuan 750021, China

ARTICLE INFO

Article history:
Received 14 August 2023
Revised 2 September 2023
Accepted 11 September 2023
Available online 14 September 2023

Keywords:
Multinuclear Co^{II}-clusters
Disk-like motif
Structural modulation
Ferromagnetic coupling
Zero-field SMM

ABSTRACT

Concise chemistry leads to a family of heptanuclear Co^{II}-clusters, $[Co_7(N_3)_{12}(CH_3CN)_{12}][Y_2(NO_3)_4(piv)_4]\cdot 2CH_3CN$ (**DC1**) (pivH = pivalic acid), $[Co_7(N_3)_{12}(CH_3CN)_{10}(NO_3)_{0.4}(Cl)_{1.6}]\cdot 4CH_3CN$ (**DC2**) and $[Co_7(N_3)_{12}(CH_3CN)_{10}(NO_3)_2]\cdot 4CH_3CN$ (**DC3**), in which the metal ions are exclusively bridged by end-on azido ligands to stabilize a beautiful disk-like topology. The resulting clusters exhibit interesting structural transformations and thermodynamically-distinct steady states verified by theoretical calculations. Magnetic studies reveal the first observation of zero-field SMM behaviour in disk-like heptanuclear Co^{II} complexes.

As a kind of basically structural units existing in discrete or extended systems, paramagnetic multi-metal cluster with the nuclear number over five is usually an intriguing research frontier due to their attractive motifs [1–3], prospective applications in diverse research fields, such as magnetic materials [4], optical materials [5], and catalyst [6]. Particularly, magnetic molecule, high-spin molecule [7] and single-molecule magnet (SMM) [8–11] are doubtlessly two nontrivial research fields where multinuclear 3d transition metal complexes are regarded as an indispensable constituent. One of the challenges in this field is that the currently reported 3d-metal clusters are more complex in the self-assembly process, with variable structures and poor controllability. The general synthetic approach usually offered plenty of structurally unpredictable metal clusters, such that the cognitions of the assembly process and mechanism are still ambiguous [12–16].

It is well-known that multi-spin Co^{II}-clusters have becoming appealing candidate for molecular magnetism especially for SMM, due to its significant magnetic anisotropy and large spin-orbit coupling [17–22]. However, among the reported polynuclear Co^{II}-clusters [23–25], SMM behaviour without an extra magnetic field was still difficult to be observed above 2 K [26,27]. An important reason is that the competent ferromagnetic (F) interaction is absent to give a large spin ground state, as oxygen-containing bridges usually tend to transfer antiferromagnetic (AF) coupling. It has been reported that azido (N_3^-) ligand is one of the versatile, flexible moieties in the fabrication of coordination polymers, qualified for connecting diverse metal ions and giving rise to attractive networks with remarkable magnetisms [28–31]. In principle, end-on (EO) azido bridge is capable of promoting F coupling between metal centers, thus causing SMM with spin-canting behaviour or long-range ordering [32–34].

In most known 3d-metal clusters, azido ligand has been predominantly employed in combination with other organic bridges/chelates [35,36]. Although essential for the crystallinity and thermodynamic stability of the preparing complexes, the attendance of other bridging/chelating ligands often impacts the dynamic magnetic relaxations of the resulting complexes, producing competing AF coupling, among others [37–39]. A potential strategy to overcome the problem and fabricate strong ferromagnetic system is the development of promising synthetic methods for the construction of polynuclear azido-metal clusters without requiring the coexistence of other bridging/chelating ligands [40]. Krause *et al.* suggested an exercisable solution for the assembly of structurally and magnetically impressive multinuclear Ni^{II} complexes by using Me_3SiN_3 as the azido-bridge pioneer in the absence of any bridging/chelating ligands [41–44]. Inspired by this case, we

* Corresponding author.
E-mail address: xiangyuliu432@126.com (X. Liu).

https://doi.org/10.1016/j.cclet.2023.109082
1001-8417/

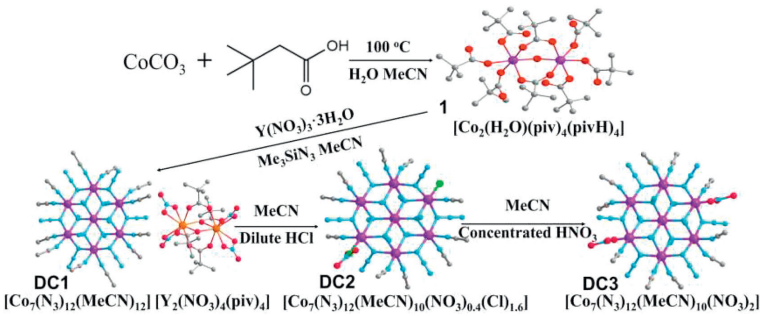

Scheme 1. Synthetic route of complexes **DC1-DC3**.

demonstrate an effective route to obtain such a unique class of ferromagnetic species, N-rich and O-free disk-like Co^{II}-clusters with the attendance of SMM behaviour in zero dc-field. More importantly, we also show that access to the structural manipulation of polynuclear Co^{II}-clusters becomes feasible through the exploration of the modulating mechanism on coordination microenvironment around terminal metal ions.

Through carefully adjusting the reaction conditions, a known complex $[Co_2(H_2O)(piv)_4(pivH)_4]$ (**1**) [45] prepared by $CoCO_3$ and pivalic acid was used to mix with $Y(NO_3)_3{\cdot}3H_2O$ in a molar ratio of 2:1 in MeCN, in excess of Me_3SiN_3, leading to a deep purple solution, which upon diffusion with Et_2O, yielded the purple crystals of a new complex $[Co_7(N_3)_{12}(CH_3CN)_{12}][Y_2(NO_3)_4(piv)_4]{\cdot}2CH_3CN$ (**DC1**) (pivH = pivalic acid), of which the crystal samples react with dilute hydrochloric acid in MeCN giving complex $[Co_7(N_3)_{12}(CH_3CN)_{10}(NO_3)_{0.4}(Cl)_{1.6}]{\cdot}4CH_3CN$ (**DC2**). Furthermore, complex $[Co_7(N_3)_{12}(CH_3CN)_{10}(NO_3)_2]{\cdot}4CH_3CN$ (**DC3**) could be yielded by dissolving the **DC2** crystals in MeCN with the addition of concentrated nitric acid (Scheme 1).

In view of such an interesting chemical process as above, it is significant to understand the formation of these complexes with the aid of theoretical calculation which can be used to explore the thermodynamic stability for **DC1-DC3**. The calculations were performed in the Vienna *ab-initio* simulation package (VASP), using DFT to exchange the correlation potential energy in the generalized gradient approximation (GGA), and the projector-augmented wave (PAW) method. To begin with, the crystallographic segment of CoN_6 for the complex, whose symmetry and structure remained unchanged, were selected as substrates, and all possible structures were further optimized with the addition and removal of small ligand molecules (Fig. S1 in Supporting information) in an attempt to find the respective optimal binding sites. The adsorption structures of three different ligand molecules CH_3CN, NO_3, and Cl species at four different positions of CoN_6 were obtained by systematically investigating various binding sites and Gibbs free energies (Figs. S2–S4 in Supporting information). Notably, the substrate energies were negative after small molecule linking, and the results all converged as expected. By comparing the Gibbs free energies of small ligand molecules at different binding sites (Table S1 in Supporting information), it is found that CH_3CN is located directly above C, whereas NO_3 and Cl were located on the C-N vertical substrate with more negative Gibbs free energies and more stable bonding. The steady state energies of **DC1-DC3** are calculated as -683.485, -646.968 and -774.086 eV, respectively. The corrected Gibbs free energy values for individual atoms are -6.624, -6.602 and -7.636 eV for **DC1**-**DC3**, respectively (Table S2 in Supporting information), yielding the differences of 0.022 eV between **DC1** and **DC2**, and 1.034 eV between **DC2** and **DC3** (Fig. 1). Thermodynamically, it is found that **DC3** is of the most steady state, **DC1** comes second place, while complex **DC2** can be considered as a thermodynamically metastable state, which corresponds to the single-crystal incubation method during the synthetic process.

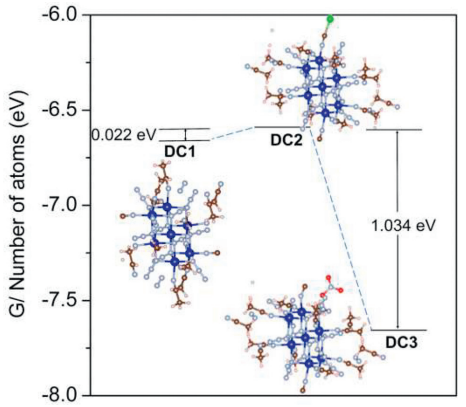

Fig. 1. Steady-state energies for **DC1-DC3**.

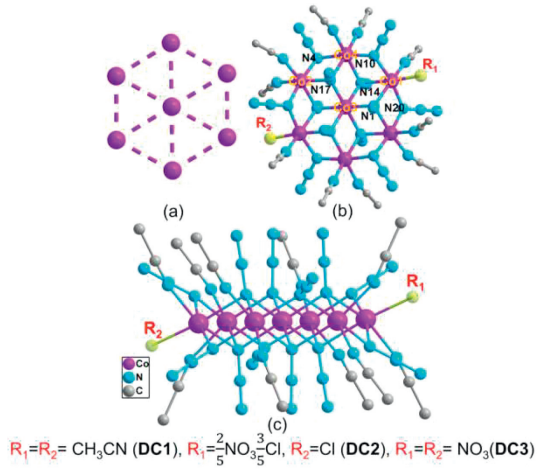

Fig. 2. (a) Representation of the Co_7 disc core. (b) Partially labeled representation of the dications and (c) a side view of complexes **DC1-DC3**. Color scheme: Co^{II} purple, N pale blue, C light gray. All hydrogen atoms were omitted for clarity.

Single-crystal structure analysis reveals that **DC1-DC3** are indicative of Co_7 disk-like unit with a highly structural similarity. All Co^{II} centers are hexa-coordinated with *quasi*-octahedral geometry. The centrosymmetric heptanuclear motif presents an ideal hexagonal plane (Fig. 2a) in which a central Co^{II} atom is surrounded by six alternating Co^{II} atoms (Fig. 2b and Fig. S5 in Supporting information). The Co_2 pairs of the hexagon are linked by six azido bridges with μ-1,1 EO mode, while the linkages between the external Co_6 hexagon and the centric Co atom are provided by six μ_3-1,1,1 EO azides. All complexes display a layer-like configuration, with N atoms from azido ligands and C atoms from acetonitrile above and below the Co_7 plane (Fig. 2c). Then, the Co_7 fragment provides a virtual C_3 symmetry. Structurally, **DC1-DC3** are

comparable to a few of previously reported disc-like Co_7 clusters [18,19,46–52].

In addition to similarities, however, there are subtle differences among these three complexes. Complex **DC1** is composed of one heptanuclear cluster $[Co_7(N_3)_{12}(MeCN)_{12}]^{2+}$, and one $[Y_2(NO_3)_4(piv)_4]^{2-}$ counter anions (Fig. S6 in Supporting information). Inorganic core of **DC1** could alternatively be regarded as composing of six $\{Co_3(N_3)_4\}$ partial cubane groups, each biface sharing, and all six vertexes sharing at the core Co^{II} ion. All Y^{III} atoms in $[Y_2(NO_3)_4(piv)_4]^{2-}$ are non-coordinated and surrounded by four O atoms from two bidentate chelating NO_3^- groups, and five O atoms from four bidentate chelating piv groups. The shortest distance between the Y^{III} ion in the $[Y_2(NO_3)_4(piv)_4]^{2-}$ counter ion and the $\{Co_7\}^{2+}$ moiety is 6.942 Å, while the intramolecular Y···Y distance is 3.818 Å. The coordination geometric spheres of all Y^{III} atoms were determined by the SHAPE 2.1 software [53] according to the crystallographic data, and the typical coordination geometries are listed in (Table S4 in Supporting information). The calculated continuous shape measures (*CShMs*) values suggest that the Y^{III} ions in **DC1** indicate the unified Muffin polyhedron with the identical *Cs* symmetry (Fig. S5). The peripheral ligation of Co_6 hexagon in **DC1** is filled with 12 terminal acetonitrile molecules, two on each of the external Co^{II} ions. For **DC2**, noteworthily, one of the peripheral Co atoms (Co1) is linked to one MeCN molecule and one chloride ion, whereas another Co1A atom is coordinated with mixed moieties of NO_3^-/Cl^- (proportion 2/3) (Fig. S7 in Supporting information). Different from **DC1** and **DC2**, external six Co atoms in **DC3** bond with ten terminal MeCN molecules and two NO_3^- groups, in which Co1 and Co1A atoms are surrounded by one MeCN molecule and one NO_3^- group, respectively (Fig. S8 in Supporting information). The peripheral Co···Co separations in **DC1-DC3** span the range 3.251–3.265 Å, 3.271–3.316 Å and 3.265–3.271 Å, and the Co-N-Co angles are in the ranges of 95.45°–103.80°, 117.597°–121.57° and 95.65°–103.72°, respectively (Tables S5–S7 in Supporting information). The stacking of the Co_7 units in **DC1-DC3** show long intermetallic distances between Co^{II} ions of adjacent molecules, with the shortest intermolecular Co···Co distances being 9.581, 8.275 and 8.294 Å, respectively (Figs. S9-S11 in Supporting information).

Direct-current (dc) magnetic data for **DC1-DC3** were collected in the 2–300 K range under 0.1 T applied field. The $\chi_M T$ values at room temperature are 23.01, 24.58 and 25.03 cm^3 K/mol for **DC1-DC3**, respectively, which are larger than the spin-only ($g=2$) values of 13.13 cm^3 K/mol expected for non-interacting Co_7 species, implying significant orbital contribution of Co^{II} cations in an octahedral symmetry [54]. Upon decreasing the temperature, the $\chi_M T$ values increase continuously, reaching the maximums of 88.43 (**DC1**) cm^3 K/mol at 18 K, 89.88 (**DC2**) and 74.80 (**DC3**) cm^3 K/mol at 7 K, before reducing to 36.35, 43.76 and 60.55 cm^3 K/mol for **DC1-DC3** at 2 K, respectively (Figs. 3a, c and e, Fig. S12 in Supporting information). This rising behaviour indicates overall F coupling between the Co^{II} ions, while the rapid decline might depend on the onset of ZFS of Co^{II}, and/or the AF intermolecular interactions, as well as the more general integrations due to spin orbital coupling (SOC), which is a common source of difficulty in the cognition of magnetism for Co^{II} species [19,55]. The temperature dependent $\chi_M{}^{-1}$ curves of three complexes above 25 K keep to the Curie–Weiss law, giving *C* of 21.9 cm^3 K/mol and θ of 18.8 K for **DC1**, *C* of 24 cm^3 K/mol and θ of 10.8 K for **DC2** and *C* of 24.1 cm^3 K/mol and θ of 13.4 K for **DC3**. The positive θ values support a predominantly intermetallic F coupling in the Co_7 cluster (Figs. 3a, c and e). In view of the coordination patterns in the heptanuclear Co cluster, the magnetic susceptibilities were tentatively simulated by a fitting model that was previously proposed by Gao for a structurally similar Co^{II} cluster with a *quasi* S_6 symmetric geometry [46]. All magnetic data was fitted by using PHI program [55], and all *J* constants are referred to the -*J* Hamiltonian. In the high-*T* (>150K) range, the fitting gives an average $J_{av}=+12.1$ cm^{-1} (**DC1**), +8.4 cm^{-1} (**DC2**) and +10.5 cm^{-1} (**DC3**) with each $S_{Co}=3/2$ and $g = 2.50$; fitting with 2*J* parameters is inclined to obtain approximate *J* values. Then, an effective spin $S'_{Co}=1/2$ system was considered in the low-*T* (2–30 K) area, obtaining an excellent fit with with $J_{av}=+33.9$ cm^{-1}, $zJ'=-0.23$ cm^{-1}, and $g=6.62$ for **DC1**, $J_{av}=+21.3$ cm^{-1}, $zJ'=-0.73$ cm^{-1}, and $g=6.58$ for **DC2**, $J_{av}=+27.2$ cm^{-1}, $zJ'=-0.48$ cm^{-1}, and $g=6.69$ for **DC3**. The results further confirm the significant intramolecular F interactions in the Co7 cluster of three complexes, which motivate an effective ground state of $S=7/2$.

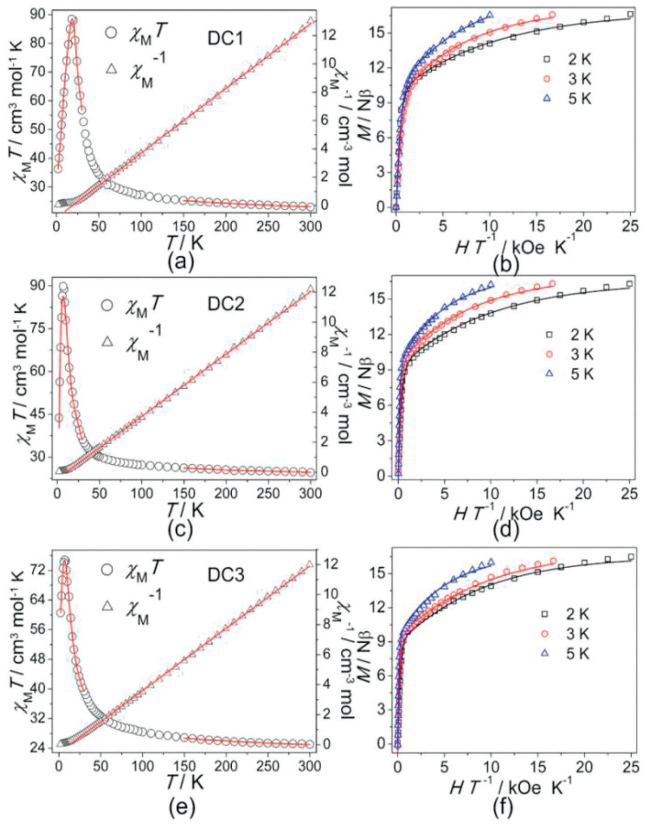

Fig. 3. Plots of $\chi_M T$ *vs.* *T* and $1/\chi_M$ *vs.* *T* for (a) **DC1**, (c) **DC2** and (e) **DC3** at $H=1$ kOe. Plots of *M vs. H/T* for (b) **DC1**, (d) **DC2** and (f) **DC3** at different temperatures. The solid lines are the best fitting.

The *M vs. H* data for **DC1-DC3** were collected up to 5 T at low temperatures (Fig. S13 in Supporting information). The sharp rise of *M* at low fields supports the existence of intracluster F couplings, then slowly reach the maximal values of 16.63 μ_B (**DC1**), 16.28 μ_B (**DC2**) and 16.49 μ_B (**DC3**) with a lack of saturation even at 2.0 K. Moreover, the non-saturated *M* values together with the non-superimposition of *M vs. H*/*T* plots (Figs. 3b, d and f) imply the occurrence of strong single-ion anisotropy, which is depending on the well-known significant SOC of the Co^{II} cation [56–59]. Fitting of the decreased *M* data is performed assuming a well-isolated, obtaining $S=7/2$ ground state with $D = -4.52, -5.08, -4.72$ cm^{-1} and $g = 6.56, 6.63, 6.59$ for **DC1**-**DC3**, respectively.

Alternating current (ac) magnetic data were measured in the absence of dc field to unravel the dynamic magnetisms of **DC1-DC3**. All complexes show explicit temperature and frequency-dependent signals for in-phase (χ') and out-of-phase (χ'') products (Figs. S14–S17 in Supporting information). Significant temperature-dependent peaks appear in the low temperature range, illustrating that the relaxation process *via* the quantum channel was clearly weaken or repressed. For frequency-dependent

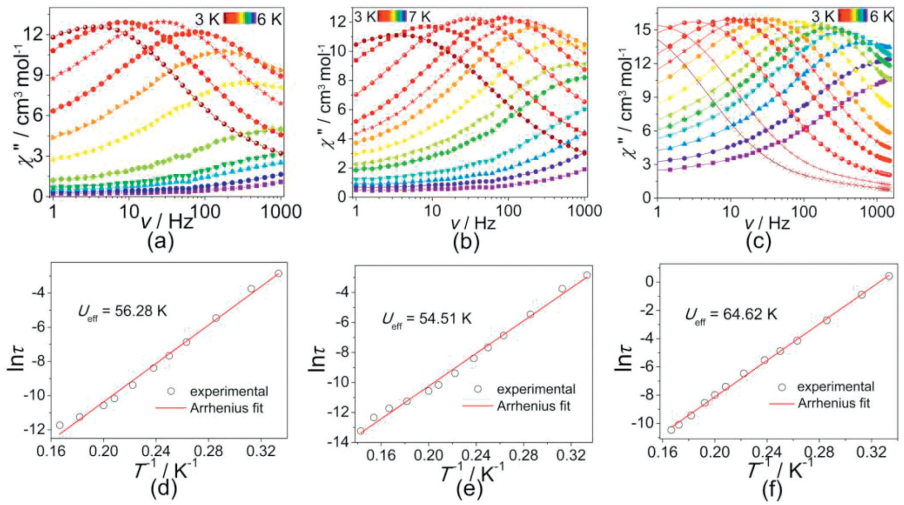

Fig. 4. $\chi''(f)$ susceptibilities for (a) **DC1**, (b) **DC2** and (c) **DC3** at 0 Oe. $\ln\tau$ *vs.* T^{-1} plots at 0 Oe for (d) **DC1**, (e) **DC2** and (f) **DC3**. The red lines represent the Arrhenius fit.

ac susceptibility with increased frequency, the maxima in χ'' plots move to high-temperature region, characteristic of a superparamagnetic behaviour (Figs. 4a–c). When **DC1-DC3** are subjected to an ac magnetic field at temperatures between 3 K and 6 K, a peak in the χ'' component and a concurrent decrease in the χ' component (Fig. S17) are observed, confirming magnetic blocking on a millisecond to second time scale. An Arrhenius fitting of $\ln(\tau)$ *vs.* T^{-1} for **DC1** (Fig. 4d) obtains $U_{\text{eff}} = 56.28$ K and $\tau_0 = 4.08 \times 10^{-10}$ s. Similar analyses yield $U_{\text{eff}} = 54.51$ K and $\tau_0 = 6.55 \times 10^{-10}$ s for **DC2**, $U_{\text{eff}} = 64.62$ K, $\tau_0 = 7.58 \times 10^{-10}$ s for **DC3** (Figs. 4e and f). This places **DC1-DC3** among the small collection of Co_7-based single molecule magnets [17–22]. The Cole-Cole curves for **DC1-DC3** are also studied at variable temperatures (Fig. S18 in Supporting information). These curves are based on a generalised Debye function, with α parameters in the ranges of 0.324–0.458 for **DC1**, 0.262–0.509 for **DC2** and 0.291–0.331 for **DC3** (Tables S8–S10 in Supporting information), signifying a wide distribution of relaxation time for the magnetic relaxations of **DC1-DC3**.

To gain further insight into the SMM behaviour, hysteresis loops were performed at different temperatures. The fields were swept from 0 T to +1.5 T and then to -1.5 T and back. The results indicate that the tiny hysteresis openings are observed at 5 K for **DC1**, 4 K for **DC2** and 2 K for **DC3** (Fig. S19 in Supporting information). Moreover, Gatteschi *et al.* emphasized that for SMM a second temperature, T_{IRREV}, should also be noticed, which is the point where the FC and ZFC curves diverge, as this is the temperature below which the magnetic observables are out-of-equilibrium and show history-dependent behaviour [60]. In this case, T_{IRREV} are observed at 5, 4 and 2 K for **DC1-DC3**, respectively, and the ZFC plots cross the FC plots (Fig. S20 in Supporting information); conventionally convergence of the two curves should appear at the maxima of the ZFC data, and the FC data should usually be larger than the ZFC one. Compared with the rarely existing disk-like Co_7 complexes, even the previously reported multinuclear Co clusters, the present three cases for the first time exhibit the slow relaxation of the magnetization at zero dc field, which is a significant enhancement of the magnetic properties for polynuclear Co-containing clusters (Table S11 in Supporting information) [18–20,46,61].

In summary, we have herein exemplified an elaborate synthetic route and structural transformation of three new disc-type heptanuclear Co^{II} clusters that are prepared by only using the flexible and versatile azido without requiring the simultaneous presence of any bridging/chelating organic liangs. Thermodynamically, **DC3** stands in the most stable state, followed by **DC1**, and **DC2** keeps in a metastable state. The overall intracluster ferromagnetic interaction contributes to a large ground state and dynamic magnetic relaxation under zero static field for three complexes. Besides the fascinating magnetic properties, investigations on the other application fields, for instance, high-energy materials due to the nitrogen-rich content, are in progress.

Declaration of competing interest

The authors declare that they have no known competing financial interests or personal relationships that could have appeared to influence the work reported in this paper.

Acknowledgments

This work was supported by the National Natural Science Foundation of China (NSFC, Nos. 21863009 and 22063008), the Natural Science Foundation of Ningxia Province (Nos. 2023AAC03014, 2023AAC03227, 2021AAC03136 and 2021BEB04062), the Young Top-notch Talent Cultivation Program of Ningxia Province, the Discipline Project of Ningxia (No. NXYLXK2017A04) and the China Postdoctoral Science Foundation (No. 2022M723148).

Supplementary materials

Supplementary material associated with this article can be found, in the online version, at doi:10.1016/j.cclet.2023.109082.

References

[1] M. Nakano, H. Oshio, Chem. Soc. Rev. 40 (2011) 3239–3248.
[2] A. Landart-Gereka, M.M. Quesada-Moreno, I.F. Díaz-Ortega, et al., Inorg. Chem. Front. 9 (2022) 2810–2831.
[3] P. Kumar Sahu, R. Kharel, S. Shome, S. Goswami, S. Konar, Coordin. Chem. Rev. 475 (2023) 214871.
[4] E. Arias-Egido, M.A. Laguna-Marco, C. Piquer, et al., Mater. Des. 196 (2020) 109083.
[5] Z. Wang, J.J. Liu, M.Y. Li, G. Chen, Chem. Eng. J. 462 (2023) 142154.
[6] B.D. Nath, K. Takaishi, T. Ema, Catal. Sci. Technol. 10 (2020) 12–34.
[7] S. Schmitz, X. Qiu, M. Gloss, et al., Front. Chem. 7 (2019) 681.
[8] G.P. Guedes, S. Soriano, N.M. Comerlato, et al., Inorg. Chem. Commun. 37 (2013) 101–105.
[9] M. Wang, Y. Guo, Z. Han, et al., Inorg. Chem. 61 (2022) 9785–9791.
[10] Q.C. Luo, N. Ge, Y.Q. Zhai, et al., Chin. Chem. Lett. 34 (2023) 107547.
[11] M. Wang, X. Meng, N. Liu, et al., Chin. Chem. Lett. 34 (2023) 107995.
[12] B.H. Wilson, J.S. Ward, D.C. Young, et al., Angew. Chem. Int. Ed. 61 (2022) e202113837.
[13] S. Mondal, A. Lunghi, J. Am. Chem. Soc. 144 (2022) 22965–22975.
[14] C.M. Liu, D.Q. Zhang, X. Hao, D.B. Zhu, Inorg. Chem. Front. 7 (2020) 3340–3351.
[15] S. Li, Z. Weng, L. Jiang, et al., Chin. Chem. Lett. 34 (2023) 107251.
[16] X.L. Li, L. Zhao, J. Wu, et al., Chem. Sci. 13 (2022) 10048–10056.

[17] Q. Chen, M.H. Zeng, Y.L. Zhou, H.H. Zou, M. Kurmoo, Chem. Mater. 22 (2010) 2114–2119.
[18] D.I. Alexandropoulos, L. Cunha-Silva, A. Escuer, T.C. Stamatatos, Chem. Eur. J. 20 (2014) 13860–13864.
[19] X.T. Wang, B.W. Wang, Z.M. Wang, W. Zhang, S. Gao, Inorg. Chim. Acta 361 (2008) 3895–3902.
[20] D.M. Chen, X.Z. Ma, X.J. Zhang, N. Xu, P. Cheng, Inorg. Chem. 54 (2015) 2976–2982.
[21] L.Q. Wei, B.W. Li, S. Hu, M.H. Zeng, CrystEngComm 13 (2011) 510–516.
[22] E.C. Yang, Z.Y. Liu, L. Zhang, N. Yang, X.J. Zhao, Dalton Trans. 45 (2016) 8134–8141.
[23] I. Radu, V.C. Kravtsov, S.M. Ostrovsky, et al., Inorg. Chem. 56 (2017) 2662–2676.
[24] D. Shao, F.X. Xu, L. Yin, et al., Chin. J. Chem. 40 (2022) 2193–2202.
[25] A. Świtlicka, B. Machura, M. Penkala, et al., Inorg. Chem. Front. 7 (2020) 2637–2650.
[26] A. Castro-Alvarez, Y. Gil, L. Llanos, D. Aravena, Inorg. Chem. Front. 7 (2020) 2478–2486.
[27] W. Wang, H. Hai, S.H. Zhang, et al., J. Clust. Sci. 25 (2013) 357–365.
[28] A. Escuer, J. Esteban, S.P. Perlepes, T.C. Stamatatos, Coordin. Chem. Rev. 275 (2014) 87–129.
[29] S. Li, Z. Weng, L. Jiang, et al., Chin. Chem. Lett. 34 (2023) 107489.
[30] Y.F. Zeng, X. Hu, F.C. Liu, X.H. Bu, Chem. Soc. Rev. 38 (2009) 469–480.
[31] J. Netz, A.O. Mitrushchenkov, A. Kohn, J. Chem. Theory Comput. 17 (2021) 5530–5537.
[32] S.F.M. Schmidt, M.P. Merkel, G.E. Kostakis, et al., Dalton Trans. 46 (2017) 15661–15665.
[33] J.K. Staab, N.F. Chilton, J. Chem. Theory Comput. 18 (2022) 6588–6599.
[34] J. Han, R. Cheng, L. Liu, H. Ohno, S. Fukami, Nat. Mater. 22 (2023) 684–695.
[35] T.C. Stamatatos, E. Rentschler, Chem. Commun. 55 (2018) 11–26.
[36] K.X. Yu, J.G.C. Kragskow, Y.S. Ding, et al., Chem. Eur. J. 6 (2020) 1777–1793.
[37] X.M. Zhang, K. Wang, Y.Q. Wang, E.Q. Gao, Dalton Trans. 40 (2011) 12742–12749.
[38] Y.S. Ding, K.X. Yu, D. Reta, et al., Nat. Commun. 9 (2018) 3134.
[39] A. Lunghi, Sci. Adv. 8 (2022) eabn7880.
[40] D. Krylov, G. Velkos, C.H. Chen, et al., Inorg. Chem. Front. 7 (2020) 3521–3532.
[41] J. Krause, D.I. Alexandropoulos, L.M. Carrella, E. Rentschler, T.C. Stamatatos, Chem. Commun. 54 (2018) 12499–12502.
[42] A.A. Athanasopoulou, M. Pilkington, C.P. Raptopoulou, A. Escuer, T.C. Stamatatos, Chem. Commun. 50 (2014) 14942–14945.
[43] P.S. Perlepe, A.A. Athanasopoulou, K.I. Alexopoulou, et al., Dalton Trans. 43 (2014) 16605–16609.
[44] A.A. Athanasopoulou, C.P. Raptopoulou, A. Escuer, T.C. Stamatatos, RSC Adv. 4 (2014) 12680–12684.
[45] V.I. Ovcharenko, O.V. Kuznetsova, Russ. Chem. Rev. 89 (2020) 1261–1273.
[46] Y.Z. Zhang, W. Wernsdorfer, F. Pan, Z.M. Wang, S. Gao, Chem. Commun. 31 (2006) 3302–3304.
[47] Y.L. Zhou, M.H. Zeng, L.Q. Wei, B.W. Li, M. Kurmoo, Chem. Mater. 22 (2010) 4295–4303.
[48] R.X. Zhao, Q.P. Huang, G. Li, et al., J. Clust. Sci. 25 (2014) 1099–1108.
[49] S.H. Zhang, Y. Song, H. Liang, M.H. Zeng, CrystEngComm 11 (2009) 865–872.
[50] M.E. Slater-Parry, J.P. Durrant, J.M. Howells, et al., Dalton Trans. 48 (2019) 1477–1488.
[51] H.L. Zheng, X.L. Chen, T. Li, et al., Chem. Eur. J. 24 (2018) 7906–7912.
[52] S.T. Meally, C. McDonald, P. Kealy, et al., Dalton Trans. 41 (2012) 5610–5616.
[53] M. Llunell, D. Casanova, J. Cirera, P. Alemany, S. Alvarez SHAPE Version 2.1, Shape Software, Barcelona, 2013.
[54] M. Kurmoo, Chem. Soc. Rev. 38 (2009) 1353–1379.
[55] N.F. Chilton, R.P. Anderson, L.D. Turner, A. Soncini, K.S. Murray, J. Comput. Chem. 34 (2013) 1164–1175.
[56] Y. Wu, J. Xi, T. Xiao, et al., Inorg. Chem. Front. 8 (2021) 5158–5168.
[57] M.R. Saber, M.K. Singh, K.R. Dunbar, Chem. Commun. 56 (2020) 8492–8495.
[58] C.E. Patrick, S. Kumar, G. Balakrishnan, et al., Phys. Rev. Lett. 120 (2018) 097202.
[59] J. Mohapatra, M. Xing, J. Elkins, J.P. Liu, J. Alloys Compd. 824 (2020) 153874.
[60] D. Gatteschi, A. Cornia, M. Mannini, R. Sessoli, Inorg. Chem. 48 (2009) 3408–3419.
[61] T.S. Mahapatra, D. Basak, S. Chand, et al., Dalton Trans. 45 (2016) 13576–13589.